



Modeling and computing throughput capacity of wireless multihop networks [☆]

Patrick Stuedi ^{*}, Gustavo Alonso

Department of Computer Science, ETH Zurich, 8092 Zurich, Switzerland

Abstract

Capacity is an important property for QoS support in Mobile Ad Hoc Networks (MANETs) and has been extensively studied. However, most approaches rely on simplified models (e.g., protocol interference, unidirectional links, perfect scheduling or perfect routing) and either provide asymptotic bounds or are based on integer linear programming solvers. In this paper, we present a probabilistic approach to capacity calculation by linking the normalized throughput of a communicating pair in an ad hoc network to the connection probability of the two nodes in a so-called *schedule graph* $G_T(\mathcal{N}, \mathcal{E})$. The effective throughput of a random network is modeled as a random variable and its expected value is computed using Monte-Carlo methods. A schedule graph $G_T(\mathcal{N}, \mathcal{E})$ for a given network is directly derived from the physical properties of the network like node distribution, radio propagation and channel assignment. The modularity of the approach leads to a capacity analysis under more realistic network models. In the paper, throughput capacity is computed for various forms of network configurations and the results are compared to simulation results obtained with ns-2.

© 2007 Elsevier B.V. All rights reserved.

Keywords: Ad hoc networks; Throughput capacity

1. Introduction

Capacity is typically studied by choosing a network model that facilitates analytical treatment. In doing so, the problem has to be simplified by either making assumptions about the network

(e.g., symmetric links), radio propagation (e.g., isotropic signal propagation, protocol interference) or the size of the network (e.g., very large number of nodes). In this paper, we eliminate many of these restrictions by looking at throughput capacity from a probabilistic perspective. Since the capacity of random networks must be random as well, we model the achievable throughput per communication pair in a multihop wireless network as a random variable. The approach is centered around a so-called *schedule graph* $G_T(\mathcal{N}, \mathcal{E})$ which is directly derived from the physical properties of the network. The effective throughput capacity of a pair of nodes in an

[☆] The work presented in this paper was supported (in part) by the National Competence Center in Research on Mobile Information and Communication Systems (NCCR-MICS), a center supported by the Swiss National Science Foundation under Grant Number 5005-67322.

^{*} Corresponding author.

E-mail addresses: stuedip@inf.ethz.ch (P. Stuedi), alonso@inf.ethz.ch (G. Alonso).

ad hoc network is then shown to be related to the connection probability of these two nodes in $G_T(\mathcal{N}, \mathcal{E})$. Due to its modularity, our approach is decoupled from specific network properties such as the channel multiplexing scheme, the signal propagation and interference model, the routing, or the node distribution. Thus, our approach can be seen as a powerful tool to analyze any form of interaction between the physical and logical properties of the network with regard to throughput capacity.

1.1. Related work

Capacity and scheduling issues have been a focus of research for many years [9,7,12]. In contrast to the consensus that accurate physical layer models are important [3,21,25,1], many recent studies are still based on a simplified interference model such as the protocol model. In [6], the authors use the protocol model to investigate the interaction between channel assignment and distributed scheduling in multi-channel, multiradio wireless mesh networks. Broadcast capacity of multihop wireless networks under protocol interference is studied in [10]. The k -hop interference model is an extension of the traditional protocol model in that it considers all nodes within a hop distance of k from the receiver as interfering nodes. Such a model is studied in [19] to derive bounds for the scheduling complexity. The relation between the k -hop neighborhood and the set of interfering nodes, however, is not clear. An interference model similar to the disk model described in this work is used in [14]. The authors describe an improved packet scheduling algorithm based on virtual coordinates. In [24], the authors also use a disk-based interference model but their work allows for different transmission and interference range settings per node. In their seminal work [9], Gupta and Kumar have studied capacity asymptotically for an increasing node density. They have shown that the throughput capacity $\lambda(n)$ for a network of n nodes within an area of $[0, 1]^2$ is in the order of $\Theta(1/\sqrt{n \log n})$. However, asymptotic analysis typically omits the constant factor that determines whether a realistic and finite network will have a useful per node throughput. Recently, there has been some effort to compute concrete throughput values [2,4,23] using integer linear programming (ILP). However, ILP makes it very difficult to model physical net-

work properties such as realistic signal propagation, link asymmetry or interference. There is some work on capacity trying to use more realistic network assumptions. In [8], the result in [9] was extended for models including variable transmission power. Bound attenuation functions and multiple channels are studied in [7,12]. Joint congestion control and resource allocation, also under physical interference, has been investigated in [20]. One of the first approaches to apply combined topology control and channel assignment algorithms to SINR-based interference models in multi-hop wireless networks can be found in [15]. A fast scheduling algorithm for the physical interference model is proposed in [5]. Similar to interference, an accurate modeling of signal propagation is fundamental when computing capacity in wireless networks. Effects of shadowed radio propagation on the packet success probability of a fixed distance link have been analyzed in [26]. In such networks, any variation in the signal pattern impacts the perceived interference at a given node. Non-deterministic variation of signal power may further lead to link asymmetry. This behavior was measured experimentally in [1]. IEEE 802.11, the MAC protocol often mentioned in combination with ad hoc networks, allows for data transmission only if there exists a bi-directional connection between the two communicating nodes since data packets need to be acknowledged by the receiving node. Effects of asymmetric links on higher network layers were investigated in [25].

1.2. Contribution

The contributions of this paper are as follows:

- The paper presents an abstract model to compute throughput capacity in multihop wireless networks. By combining the model with Monte-Carlo methods, the paper proposes a new way of throughput capacity computation for more realistic network configurations with complex random properties. Our approach of first transforming the physical properties of the network into a graph representation has two advantages: it makes the actual throughput computation independent of low level network details and at the same time facilitates the analysis of various physical and logical effects with regard to throughput capacity.

- By linking throughput capacity of multihop wireless networks with the connection probability in a *schedule graph* $G_T(\mathcal{N}, \mathcal{E})$, the paper proposes a way of analyzing capacity in sparse and partially disconnected random networks. This might be particularly helpful with regard to throughput calculations in mobile scenarios where the movement of the nodes often leads to temporarily broken paths.
- The paper further presents and discusses an algorithm for a conflict-free channel assignment under arbitrary interference models, including *SINR*-based interference.

2. Network model

As a first step, we turn the physical properties of wireless multihop networks into a so-called *schedule graph* $G_T(\mathcal{N}, \mathcal{E})$. Examples of physical properties are node locations or perceived signal strengths. In a schedule graph, \mathcal{N} is the set of nodes in the network and \mathcal{E} denotes a set of directed edges between the nodes such that the existence of a sequence of nodes n_0, n_1, \dots, n_k – with $n_i \in \mathcal{N} \forall i \leq k$ and $(n_i, n_{i+1}) \in \mathcal{E} \forall i < k$ – states that there is also a schedule of channel assignments $\psi(n_0, n_1), \psi(n_1, n_2), \dots, \psi(n_{k-1}, n_k)$ such that node n_0 is able to consecutively transmit data to node n_k at a rate $\lambda_{n_0, n_k} > 0$. The idea behind building a schedule graph is to create an abstraction that allows us to – later on – reason about the achievable capacity of the underlying wireless network. In this section, we first define some common properties in order to then gradually develop the graph representation by assigning two sets $\mathcal{D}_n \supseteq \mathcal{U}_n$ of nodes to each node n , with $\mathcal{D}_n \subseteq \mathcal{N}$. Nodes within the particular sets correspond to the different forms of interaction nodes can have, such as unidirectional and bi-directional communication. A list of all the notations used in this paper, including the aforementioned sets of nodes, can be found in [Table 1](#).

We parameterize the network using the following five properties: The set of N nodes \mathcal{N} , a node distribution δ , a signal propagation ϑ , a channel assignment ψ and an interference model κ . We assume $x_n \in \mathcal{R}^2$ to be the coordinate¹ of node n , identifying the node's position with respect to an area \mathcal{A} , and we consider the set \mathcal{N} of nodes as being distributed

in \mathcal{A} according to some probability function $\delta : \mathcal{A} \rightarrow [0, 1]$. Throughout this paper, we use $\mathcal{P}(\cdot)$ to refer to the collection of all possible subsets of a set.

Let us start by defining how signals are propagated. A node n in the network is supposed to transmit with a signal power $P_n^t \in [0, \infty[$. We use the tuple notation (n', n) to refer to the transmission from a node n' to a node n . For a certain signal propagation function ϑ , $P_{n \leftarrow n'} = \vartheta(P_{n'}^t, |x_{n'} - x_n|) \in [0, P_{n'}^t]$ denotes the power of the received signal at node n due to the transmission (n', n) . In the simplest case, ϑ is a direct function of the distance. The path loss radio propagation model, for example, defines $\vartheta_p(p, l) = p \cdot (l/l_0)^{-\rho}$ for some path loss exponent ρ , and l_0 as a reference distance for the antenna far-field. A more sophisticated model is the log-normal shadowing radio propagation [18]:

$$\vartheta_{sh}(p, l) = p \cdot (l/l_0)^{-\rho} \cdot 10^{X/10} \quad (1)$$

where X is a gaussian random variable with zero mean and standard deviation σ and ρ is the aforementioned path loss exponent. In case of σ equal 0, there is no random effect and $\vartheta_{sh} \equiv \vartheta_p$. In this work, we assume the physical signal propagation to be symmetric. Thus, the gaussian random variable X involved in the computation of $P_{n \leftarrow n'}$ is the same as the one involved in the computation of $P_{n' \leftarrow n}$. From practical measurements, however, it is known that the signal strengths $P_{n \leftarrow n'}$ and $P_{n' \leftarrow n}$ (corresponding to transmissions of two identical radio transmitters) may not always be equal. This is due to tiny differences of the radio hardware and is taken into account in our model by the power distribution P_n^t .

Whether a signal from a node n' can be decoded correctly at node n in the absence, or the presence, of concurrent transmissions, is determined by the interference model. In the literature, two main interference models have been proposed [9]: the *protocol* and the *physical* interference model. In the protocol model, a transmission from a node n' is said to be received successfully by another node n if no node n'' closer to the destination node is transmitting simultaneously. However, in practice, nodes outside the interference range of a receiver might still cause enough cumulative interference to prevent the receiver from decoding a message from a given sender. This behavior is captured by the physical model,

¹ The model could also be applied to \mathcal{R}^3 .

² Therefore $P_n^t \equiv P_{n'}^t \Rightarrow P_{n \leftarrow n'} \equiv P_{n' \leftarrow n}$.

Table 1
Mathematical notations

Symbol	Semantic
Parameters for $G_T(\mathcal{N}, \mathcal{E})$	
\mathcal{N}	Set of nodes in the network
δ	Node distribution function
ϑ	Signal Propagation function
ψ	Channel assignment function
κ	Interference model
$G_T(\mathcal{N}, \mathcal{E})$ internal	
X	Set of coordinates x_n for each node n
Γ	Set of channels
P_n^t	Transmission power of node n
$P_{n \leftarrow n'}$	Signal power perceived at node n due to the transmission of node n'
P_n^*	Thermal noise perceived at node n
\mathcal{D}_n	Set of nodes that can be decoded at node n without noise
\mathcal{U}_n	Set of nodes that can be decoded at node n under noise
\mathcal{E}	Set of directed edges in a <i>schedule graph</i>
Parameters for λ	
$G_T(\mathcal{N}, \mathcal{E})$	Schedule graph
$\omega(n', n)$	Weight function indicating the number of channels used on a link
Υ	Set of source destination pairs
η	Routing function
λ internal	
Π	Set of paths participating in communication
$B_{n', n}$	Lowest number of channels between any two neighbors along a path
T	Used channels, $T = \Gamma $ in $G_T(\mathcal{N}, \mathcal{E})$
$\zeta_{n', n}$	Achievable throughput capacity along a path
λ	Expected throughput capacity

where a communication between nodes n' and n is successful if the SINR (Signal to Interference and Noise Ratio) at v (the receiver) is above a certain threshold.

In this work, we assume interference models to be defined by a binary interference function $\kappa : \mathcal{N} \times \mathcal{N} \times \mathcal{P}(\mathcal{N}) \rightarrow \{0, 1\}$ with

$$\kappa(n', n, \mathcal{I}) = \begin{cases} 1 & \text{The signal of } n' \text{ can be} \\ & \text{decoded at node } n \\ & \text{under a set } \mathcal{I} \text{ of interferers} \\ 0 & \text{otherwise.} \end{cases} \quad (2)$$

The interference function for the protocol model [9] is

$$\kappa_{\text{protocol}}(n', n, \mathcal{I}) = 1 \iff d(n'', n) > d(n', n) \quad \forall n'' \in \mathcal{I}. \quad (3)$$

For the physical interference model [9], the interference function is

$$\kappa_{\text{sinr}}(n', n, \mathcal{I}) = 1 \iff \frac{P_{n \leftarrow n'}}{P_n^* + \sum_{n'' \in \mathcal{I}} P_{n \leftarrow n''}} > \beta_{\text{sinr}}, \quad (4)$$

for some threshold β_{sinr} and P_n^* as the thermal noise perceived at node n .

We now assign two sets of nodes to each node $n \in \mathcal{N}$, namely, \mathcal{D}_n and \mathcal{U}_n ,

$$\mathcal{D}_n = \{n' \in \mathcal{N} \mid \kappa(n', n, \emptyset) = 1\} \quad (5)$$

is the set of nodes that can be correctly decoded at node n in the absence of any other concurrent transmission,

$$\mathcal{U}_n = \{n' \in \mathcal{D}_n \mid \kappa(n', n, I_{n'}) = 1\} \quad (6)$$

contains all nodes n' that can be correctly decoded at node n in the presence of a set of nodes $I_{n'}$ transmitting concurrently as node n' . For later use we define $\mathcal{D} = \{(n', n) \mid n' \in \mathcal{D}_n\}$ to be the set of transmissions in the network when interference is ignored, and $\mathcal{U} = \{(n', n) \mid n' \in \mathcal{U}_n\}$ to be the set of transmissions in the network if interference is considered.

3. Scheduling

Which transmissions in the network occur simultaneously is determined by the scheduling algorithm. In our model, we assume the medium to be divided into a set of channels T . Each channel $\psi_i \in T$ can be seen as a set of directed transmissions (n', n) , with $n' \in \mathcal{D}_n$, between two nodes n' and n . For the sake of simplicity, we use $\psi(n', n)$ to refer to the set of channels used by the transmission (n', n) . We further use $\psi^*(n) = \bigcup_{n': n \in \mathcal{D}_{n'}} \psi(n', n')$ to refer to all the channels where node n acts as a transmitter.

Scheduling transmissions in multi-hop wireless networks so that no two transmissions scheduled within the same channel interfere, is trivial for the protocol model, but turns out to be more difficult under the physical interference model. In general, the problem of scheduling is related to the traditional graph coloring problem, except that the vertices in the graph to be colored refer to the transmissions in the network and the edges in the graph refer to the interference conflicts. Two vertices conflict if their corresponding transmissions cannot be scheduled simultaneously. We call such a graph a *conflict graph*.

Under the physical interference model (Eq. (4)), conflicts between two transmissions cannot be determined without considering all other transmissions. As an example, two nodes n'' and n''' may interfere with a transmission from node n' to node n , even if node n cannot successfully decode the signals of either n'' or n''' in the absence of interference. For a node n' to belong to \mathcal{U}_n , $\kappa_{\text{physical}}(n', n, \mathcal{N} \setminus \mathcal{C}_{n \leftarrow n'})$ must compute to 1, given $\mathcal{C}_{n \leftarrow n'}$ contains all nodes n'' acting as a sender in a transmission that conflicts with the transmission (n', n) . In practice, of course, one wants to find the minimum set $\mathcal{C}_{n \leftarrow n'}$ of conflicts for a transmission (n', n) because this minimizes the number of channels to be used at a later point in time. How to compute the minimum set of conflicts for a given set of transmissions \mathcal{D} in the physical interference model is shown in Algorithm 1. For a given transmission (n', n) , the algorithm operates by gradually testing the SINR ratio with an increasing set of interferers, starting with the node contributing the lowest signal power. At the point where the cumulated interference of a node n'' leads to a SINR ratio smaller than β_{SINR} , all transmitting nodes n''' with $P_{n \leftarrow n''} \geq P_{n \leftarrow n''}$ are considered as interferers and their associated transmissions are defined as conflicts with (n', n) .

Algorithm 1. Conflict graph under physical interference

Input: Set of all transmission \mathcal{D}
 Output: Set of conflicts $\mathcal{C} \subseteq \{(e, e') | e, e' \in \mathcal{D}\}$

```

1:  $\mathcal{C} := \emptyset$ ;
2: for all  $e := (n', n) \in \mathcal{D}$  do
3:    $L := \text{sort}(\mathcal{N} \setminus \{n', n\})$  such that  $n'' \prec n''' \leftrightarrow P_{n \leftarrow n''} < P_{n \leftarrow n'''}$ 
4:    $\mathcal{M}^* := \emptyset$ ;
5:   for all  $n'' \in L$ 
6:      $\mathcal{M}^* := \mathcal{M}^* \cup \{n''\}$ 
7:     if  $\kappa_{\text{SINR}}(n', n, \mathcal{M}^*) = 0$  then
8:        $\mathcal{Q} := \{(n'', n''') | n'' \in \mathcal{D}_n\}$ 
9:       for all  $e' \in \mathcal{Q}$  do
10:         $\mathcal{C} := \mathcal{C} \cup \{(e', e), (e, e')\}$ ;
11:       end for
12:     end if
13:   end for
14: end for
    
```

We have shown how a conflict graph can be built for the physical interference model. Based on the conflict graph, efficient coloring algorithms might be used to assign channels to the transmissions (represented as nodes in the conflict graph). Finding the minimum number of channels, however, is an NP hard problem and thus is not feasible for large networks [11,17]. We decided to apply a *Greedy* channel assignment algorithm. Algorithm 2 assigns channels to transmissions in a greedy

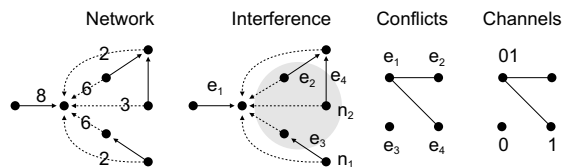


Fig. 1. Channel assignment under physical interference. The straight line arrows represent the transmissions. The dotted arrows denote signals which contribute to the interference noise of transmission e_1 . The weight assigned to an edge corresponds to the signal strength. We assume the thermal noise P^* used in Eq. (4) to be 1. According to Algorithm 1, nodes in the grey area are considered as the smallest set of nodes such that the remaining cumulative interference does not prohibit transmission e_1 from being established. There is no conflict between transmissions e_1 and e_3 because node n_1 is not included in the grey area. Note that both conflict graph and channel assignment are considered as snapshots from the perspective of e_1 .

way, so that no two transmissions e_1, e_2 will be scheduled using the same channel if there exists a conflict between the two transmissions $((e_1, e_2) \in \mathcal{C})$. **Algorithm 2** further assigns channels in a traffic proportional way, meaning that each node pair (n', n) , with $n' \in \mathcal{D}_n$, is assigned exactly as many channels as there are flows occupying the wireless link. The function $\mu(\cdot)$ in **Algorithm 2** refers to the number of flows of a link. Conflict graph and channel assignment for the physical interference model are illustrated in **Fig. 1** in a small example network.

Algorithm 2. Greedy channel assignment

Input: Set of all transmission \mathcal{D} , set of conflicts \mathcal{C}

Output: Set of channels $\{\psi_0, \psi_1, \dots, \psi_{T-1}\}$ with $\psi_i \subseteq \mathcal{D}$

```

1: for all  $e \in \mathcal{D}$  do
2:   for  $i:=0; i < \mu(e)$  do
3:      $\mathcal{Q} := \{e' | (e, e') \in \mathcal{C}\}$ 
4:      $\Omega := \emptyset$ ;
5:     for all  $e' \in \mathcal{Q}$  do
6:        $\Omega := \Omega \cup \{\psi_j | e' \in \psi_j\}$ 
7:     end for
8:      $k := \text{freechannel}(\Omega)$ ;
9:      $\psi_k := \psi_k \cup \{e\}$ ;
10:  end for
11: end for

```

freechannel(\mathcal{Q})

```

1:  $\Omega^* := \text{sort}(\mathcal{Q})$  such that  $\psi_i \prec \psi_j \leftrightarrow \text{id}\psi_i < \text{id}(\psi_j)$ 
2:  $i := -1$ 
3: for all  $\psi \in \Omega^*$  do
4:   if  $\text{id}(\psi) > i + 1$  then
5:     break;
6:   end if
7:    $i := \text{id}(\psi)$ ;
8: end for
9: return  $i + 1$ ;

```

4. Schedule graph

Coming back to the definition of \mathcal{U}_n , we can say that a node n' belongs to \mathcal{U}_n if $I_{n'}$ in Eq. (6) is defined as the set of nodes transmitting in the same channel as node n' . Given a schedule and the set \mathcal{U}_n for each node, we define a so-called schedule graph as a directed and weighted graph $G_T(\mathcal{N}, \mathcal{E})$, where \mathcal{E} denotes the set of directed edges with

$$\mathcal{E} = \{(n', n) \in \mathcal{N} \times \mathcal{N} | n' \in \mathcal{U}_n \wedge n \in \mathcal{D}_{n'}\}. \quad (7)$$

The set \mathcal{E} includes all transmissions (n', n) whose signals can be decoded correctly at node n under interference, while the reverse signal might only be correctly decoded if there is no interference. Note that Eq. (7) models the acknowledgment as an infinitely small packet not occupying the medium. The subscript T indicates the number of channels used (**Algorithm 2**). The weight of an edge $(n', n) \in \mathcal{E}$ is given by $\omega(n', n)$,

$$\omega(n', n) = \sum_{\gamma \in \mathcal{I}_\gamma(n', n)} \kappa(n', n, I_\gamma). \quad (8)$$

Here, I_γ denotes the set of nodes transmitting during channel γ , or $\mathcal{I}_\gamma = \{n' \in \mathcal{N} | \gamma \in \psi^*(n')\}$.

It follows directly from the definition of a *schedule graph* $G_T(\mathcal{N}, \mathcal{E})$ that for any path n_0, n_1, \dots, n_k – with $n_i \in \mathcal{N} \forall i \leq k$ and $(n_i, n_{i+1}) \in \mathcal{E} \forall i < k$ – there is also a corresponding schedule of channel assignments $\psi(n_0, n_1), \psi(n_1, n_2), \dots, \psi(n_{k-1}, n_k)$ in a way that node n_0 is able to consecutively transmit data to node n_k at a rate strictly greater than zero. We will make use of this property later on to reason about the achievable capacity of the underlying physical network.

5. Throughput capacity

Throughout this section, an ad hoc network is represented by its *schedule graph* $G_T(\mathcal{N}, \mathcal{E})$ and the corresponding weight function ω . Capacity is then defined over a set \mathcal{T} of communication pairs,

$$\mathcal{T} \subseteq \{(n', n) \in \mathcal{N} \times \mathcal{N} | n' \neq n\}. \quad (9)$$

More precisely, we say that a *schedule graph* $G_T(\mathcal{N}, \mathcal{E})$ with a communication pattern \mathcal{T} has a throughput capacity of $\lambda_{n', n}$ if a communication pair $(n', n) \in \mathcal{T}$ can expect an end-to-end throughput of $\lambda_{n', n}$ bits per second. Important to the computation of throughput capacity is the routing function $\eta : \mathcal{N} \times \mathcal{N} \rightarrow \mathcal{P}(\mathcal{E})$. Hence, for a given source–destination pair (n', n) the resulting route simply consists of the set³ of edges included in the sequence e_0, e_1, \dots, e_{k-1} , with $e_i = (n_i, n_{i+1}) \in \mathcal{E}, n_0 = n'$ and $n_k = n$.

³ In practice, a route would be modeled as a sequence rather than as a set, however, since we assume no loops and the order of the edges in a route is not important for the computation of λ we prefer the set notion which simplifies further treatment.

We now want to analyze the expected throughput λ of a communication pair $(n', n) \in \mathcal{Y}$. Since both the network and its graph representation $G_T(\mathcal{N}, \mathcal{E})$ are random, obviously the resulting throughput per node pair can also be considered to be random. Based on this, the approach we follow is of a probabilistic nature. For any node pair $(n, n') \in \mathcal{Y}$, we model throughput capacity as a random variable $\zeta_{n',n} : \mathcal{P}(\mathcal{Y}) \rightarrow [0, \infty[$ to then compute the expected value $E[\zeta_{n',n}]$ of $\zeta_{n',n}$, with $E[\zeta_{n',n}] = \lambda_{n',n}$. Consider the fact that in a *schedule graph*, a path between two nodes also reflects a schedule of channels. Throughput capacity is a concave metric, meaning that the available throughput for a certain source destination pair is always determined by the node with the lowest bandwidth, the so-called bottleneck. Hence, let $B_{n',n}^* = \min_{e \in \eta(n',n)} \omega(e)$ be a random variable indicating lowest number of channels available between two nodes along the path from n' to n . One can easily verify that the resulting throughput capacity along the path cannot be bigger than $W \cdot B_{n',n}^*/T$, where W is the maximum transmission rate equal to all nodes and $T = |\Gamma|$ is the number of channels used in total. The throughput capacity may however be further diminished when considering all the traffic \mathcal{Y} taking place in the network. For this purpose let us define a so-called load function $\mu : \mathcal{E} \rightarrow [0, N]$, indicating to what extent a certain edge $e \in \mathcal{E}$ is shared with other ongoing traffic, or, more formally:

$$\mu(e) = \sum_{i=\eta(n',n)(n',n) \in \mathcal{Y}} 1_i(e) \quad (10)$$

where $1_i : \mathcal{E} \rightarrow \{0, 1\}$ is the set membership function. If we want to take all ongoing traffic into account we therefore have to consider μ while computing $B_{n',n}^*$, or

$$B_{n',n} = \begin{cases} 0 & \eta(n', n) = \emptyset \\ \min_{e \in \eta(n',n)} \frac{\omega(e)}{\mu(e)} & \text{otherwise.} \end{cases} \quad (11)$$

Based on the definition of $B_{n',n}$ we now claim that the achievable throughput $\zeta_{n',n}$ for a communication pair $(n', n) \in \mathcal{Y}$ in a *schedule graph* $G_T(\mathcal{N}, \mathcal{E})$ can be modeled as

$$\zeta_{n',n} = \frac{W \cdot B_{n',n}}{T}. \quad (12)$$

In a simplified setup, where each node is only allowed to transmit within one single channel, $B_{n',n}$ refers to the path availability between n' and n in

$G_T(\mathcal{N}, \mathcal{E})$ and therefore $\zeta_{n',n}$ can be seen as a direct function of the connection probability between the two nodes. Or one can say that the capacity of an ad hoc network is related to the connectivity of its corresponding *schedule graph* $G_T(\mathcal{N}, \mathcal{E})$. This might be of interest when analyzing capacity in sparse and partially disconnected random networks, but also in mobile scenarios where the movement of the nodes often leads to temporarily broken paths.

In the following sections we show how $\lambda_{n',n} = E[\zeta_{n',n}]$ can be computed using Monte-Carlo methods.

5.1. Computing $\lambda_{n',n}$ using Monte-Carlo methods

One could compute $E[\zeta_{n',n}]$ given the common density function $p(\zeta_{n',n})$ for the random variables $\zeta_{n',n}$. However, finding the density function $p(\zeta_{n',n})$ is not trivial. In fact, the problem can be viewed as an extension to the traditional connectivity problem where one tries to find the probability of whether a given node distribution and transmission range result in a connected network. In this paper, we do not pursue an analytical treatment of $E[\zeta_{n',n}]$ but rather use a Monte-Carlo estimator. For this purpose we first generalize our model $\zeta_{n',n}$ to also reflect the average throughput capacity $\zeta = \frac{1}{|\mathcal{Y}|} \sum_{(n',n) \in \mathcal{Y}} \zeta_{n',n}$ that can be expected in the network. In fact, due to the linearity of the expected value, one can easily verify that $E[\zeta_{n',n}] = E[\zeta]$, namely,

$$\begin{aligned} E[\zeta] &= E\left[\frac{1}{|\mathcal{Y}|} \sum_{(n'',n''') \in \mathcal{Y}} \zeta_{n'',n'''}\right] \\ &= \frac{1}{|\mathcal{Y}|} \sum_{(n'',n''') \in \mathcal{Y}} E[\zeta_{n'',n'''}] = E[\zeta_{n',n'}]. \end{aligned} \quad (13)$$

Hence, the expected throughput capacity $\lambda_{n',n}$ can be approximated using the Monte-Carlo method:

$$\begin{aligned} \lambda_{n,n'} = E[\zeta_{n,n'}] &= E[\zeta] = \frac{1}{|\mathcal{Y}|} \sum_{(n'',n''') \in \mathcal{Y}} E[\zeta_{n'',n'''}] \\ &= \frac{1}{|\mathcal{Y}|} \sum_{(n'',n''') \in \mathcal{Y}} \int_{\mathcal{X}^{2N}} E[\zeta_{n'',n'''} | X] \\ &= X^*]f(X^*)dX^* \\ &\approx \frac{1}{|\mathcal{Y}|} \sum_{(n'',n''') \in \mathcal{Y}} \frac{1}{k} \sum_{i=0}^{k-1} E[\zeta_{n'',n'''} | X = X_i^*] \\ &= \frac{1}{|\mathcal{Y}|} \sum_{(n'',n''') \in \mathcal{Y}} \frac{1}{k} \sum_{i=0}^{k-1} \zeta_{n'',n'''} |_{X=X_i^*} \end{aligned} \quad (14)$$

In other words, we approximately compute the expected value of ζ for a given set of parameters by sampling over k realizations of the underlying random network, with X_i^* as a concrete set of node placements in the area \mathcal{A} .

6. Capacity of static networks

To validate the model, we compute the throughput capacity of two simple, static scenarios, static in the sense that the network topology as well as the communication pattern is fixed. The throughput of such fixed network configurations can be seen as the conditional expected value $E[\zeta|X]$ of the random variable ζ under a concrete node placement X . For a

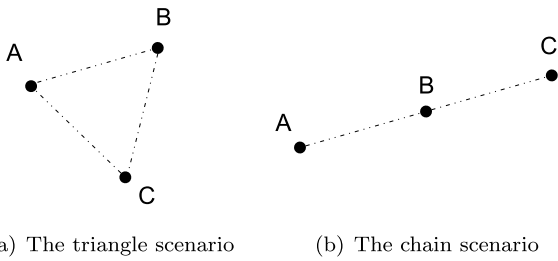


Fig. 2. Static topologies.

fixed channel assignment ψ , $E[\zeta|X]$ simply computes as $E[\zeta|X] = \frac{1}{|\mathcal{T}|} \sum_{(n',n) \in \mathcal{T}} \zeta_{n',n} |_{X=X_i^*}$, where X_i^* is the given set of coordinates of the nodes. For both examples we will consecutively derive $E[\zeta|X]$ by going through the basic steps of Sections 2 and 5.

The first network topology we consider consists of three nodes being distance d apart from each other, as shown in Fig. 2a. To simplify the analysis, we use the more primitive protocol interference model as described in Eq. (3). Let us further assume $n' \in D_n$ for all $n' \neq n$. According to κ_{protocol} , the set of senders \mathcal{U}_n is modeled in a way that a node n' belongs to \mathcal{U}_n if, and only if, no other concurrent transmission with a signal stronger than $P_{n-n'}$ is received by node n . Hence, the graph G_T only depends on how the different channels are assigned to the nodes. We now want to illustrate the outcome of $E[\zeta|X]$ for three possible channel assignments. We keep track of all states and sets of the network model for each of the three channel assignments in Table 2.

In all the configurations we assume shortest path routing and only assign channels to edges that are also used when considering the traffic pattern Υ . In the case of one common channel $\psi(n', n) = \psi(n, n')$ for all nodes n, n' , no transmission can

Table 2
States for the triangle scenario

T	$\psi(n', n)$	\mathcal{U}_n	Υ	$B_{n,n'}$	$E[\zeta X]$
1	$\psi(B, A) = \emptyset$ $\psi(C, B) = \emptyset$ $\psi(A, C) = \emptyset$ $\psi(A, B) = \{0\}$ $\psi(B, C) = \{0\}$ $\psi(C, A) = \{0\}$	\emptyset	(A, B) (B, C) (C, A)	0	0
2	$\psi(B, A) = \emptyset$ $\psi(C, B) = \emptyset$ $\psi(A, C) = \emptyset$ $\psi(A, B) = \psi(C, A) = \{0\}$ $\psi(B, C) = \{1\}$	$\mathcal{U}_A = \emptyset$ $\mathcal{U}_B = \emptyset$ $\mathcal{U}_C = \{B\}$	(A, B) (B, C) (C, A)	$B_{A,B} = 0$ $B_{B,C} = 1$ $B_{C,A} = 0$	1/6W
3	$\psi(B, A) = \emptyset$ $\psi(C, B) = \emptyset$ $\psi(A, C) = \emptyset$ $\psi(A, B) = \{0\}$ $\psi(B, C) = \{1\}$ $\psi(C, A) = \{2\}$	$\mathcal{U}_A = \{C\}$ $\mathcal{U}_B = \{A\}$ $\mathcal{U}_C = \{B\}$	(A, B) (B, C) (C, A)	$B_{A,B} = 1$ $B_{B,C} = 1$ $B_{C,A} = 1$	1/3W
4	$\psi(B, A) = \emptyset$ $\psi(C, B) = \emptyset$	$\mathcal{U}_A = \{C\}$ $\mathcal{U}_B = \{A\}$	(A, B) (B, C)	$B_{A,B} = 2$ $B_{B,C} = 1$	1/3W
5	$\psi(A, C) = \emptyset$ $\psi(A, B) = \{0, 1\}$ $\psi(B, C) = \{2\}$ $\psi(C, A) = \{3\}$	$\mathcal{U}_C = \{B\}$	(C, A)	$B_{C,A} = 1$	

Table 3
States for the chain scenario

T	$\psi(n', n)$	\mathcal{U}_n	\mathcal{Y}	$B_{n,n'}$	$E[\zeta X]$
2	$\psi(A, B) = \psi(C, B) = \{0\}$	$\mathcal{U}_A = \{B\}$	(A, B)	$B_{A,B} = 0$	1/6W
	$\psi(B, C) = \{1\}$	$\mathcal{U}_B = \emptyset$	(B, C)	$B_{B,C} = 1$	
	$\psi(B, A) = \emptyset$	$\mathcal{U}_C = \{B\}$	(C, A)	$B_{C,A} = 0$	
3	$\psi(A, B) = \{0\}$	$\mathcal{U}_A = \{B\}$	(A, B)	$B_{A,B} = 1$	2/9W
	$\psi(B, C) = \{1\}$	$\mathcal{U}_B = \{A\}$	(B, C)	$B_{B,C} = 1$	
	$\psi(C, B) = \psi(B, A) = \{2\}$	$\mathcal{U}_C = \{B\}$	(C, A)	$B_{C,A} = 0$	
4	$\psi(A, B) = \{0\}$	$\mathcal{U}_A = \{B\}$	(A, B)	$B_{A,B} = 1$	1/4W
	$\psi(B, A) = \{1\}$	$\mathcal{U}_B = \{A, C\}$	(B, C)	$B_{B,C} = 1$	
	$\psi(B, C) = \{2\}$	$\mathcal{U}_C = \{B\}$	(C, A)	$B_{C,A} = 1$	
			(A, C)	$B_{A,B} = 1/2$	1/6W
			(B, C)	$B_{B,C} = 1/2$	
			(C, A)	$B_{C,A} = 1$	
5	$\psi(A, B) = \{0\}$	$\mathcal{U}_A = \{B\}$	(A, C)	$B_{A,B} = 1$	1/5W
	$\psi(B, A) = \{1\}$	$\mathcal{U}_B = \{A, C\}$	(B, C)	$B_{B,C} = 1$	
	$\psi(B, C) = \{2,3\}$	$\mathcal{U}_C = \{B\}$	(C, A)	$B_{C,A} = 1$	
	$\psi(C, B) = \{4\}$				

correctly be decoded at any receiver (Eq. (3)) which leads to $\mathcal{U}_n = \emptyset, \mathcal{E} = \emptyset, S_{n,n'} = 0, \zeta_{n,n'} = 0$ and finally to $E[\zeta|X] = 0$. In the presence of two separate channels ($T = 2$), two directed links can be established (among the potential 6). Along with a communication pattern $\mathcal{Y} = \{(A, B), (B, C), (C, A)\}$ (see Table 2), $E[\zeta|X]$ is $W \cdot 1/3 \cdot (0 + 1/2 + 0) = 1/6 \cdot W$. If transmissions are spread over three channels, $G_T(\mathcal{N}, \mathcal{E})$ becomes fully connected and $E[\zeta|X]$ equals $W \cdot 1/3 \cdot (1/3 + 1/3 + 1/3) = 1/3 \cdot W$. Adding a fourth edge, e.g., to the transmission between node A and B , does not increase the capacity any further. This is because the increase in the bottleneck ($B_{A,B} = 2$) is compensated by the increase of the total amount of used channels ($T = 4$).

The situation is slightly different for the scenario in Fig. 2b since node B acts as a router and some of its bandwidth is consumed by traffic sent from A to C . The case $T = 1$ is trivial and comparable with the corresponding case in the triangle scenario. Assigning two channels to the four edges results in two established links ($\mathcal{U}_A = \{B\}$ and $\mathcal{U}_C = \{B\}$). Considering the traffic pattern \mathcal{Y} , it is sufficient for one path to be established (e.g., $S_{B,C} = 1$) and the resulting capacity $E[\zeta|X]$ computes to $1/6 \cdot W$. Two of the three routes can be established if three channels are used ($T = 3$), which results in $E[\zeta|X] = 2/9 \cdot W$. The capacity of the given traffic pattern can be further improved by assigning one channel per transmission pair. All the routes can be established with a bottleneck of $B_{n,n'} = 1, \forall (n, n') \in \mathcal{Y}$ and $E[\zeta|X]$ equals $1/4 \cdot W$. Obviously, the same channel assignment

results in a different capacity if another traffic pattern is used, like, e.g. $\mathcal{Y} = \{(A, C), (B, C), (C, A)\}$. Since the link between node B and C is used twice, the values for $B_{A,C}, B_{B,C}$ reduce to $1/2$. For such a traffic pattern, a 5-channel assignment performs better, as shown in Table 3.

7. Capacity of larger networks

In this section, we analyze throughput capacity of various types of communication patterns and network topologies. To simplify the notation we will refer to $E[\zeta]$ as λ for the rest of the paper. For each analyzed configuration we also provide results taken from simulations with ns-2 [22] under the very same topology and communication setup. Throughout this section, we use a path loss radio propagation as defined by ϑ_{pl} and a SINR-based interference model, κ_{sinr} , as described in Eq. (4). Since we use ϑ_{pl} , the threshold for a node n' to be part of \mathcal{D}_n only depends on the distance between the two nodes. We have set P_n^* of Eq. (4) such that $n' \in \mathcal{D}_n \iff |x_{n'} - x_n| \leq 250$. To avoid mixing up capacity measurements with routing issues, packets within ns-2 simulations are forwarded using pre-computed shortest path routes. We further have set the MAC data rate in ns-2 to 1 Mbit/s. This is necessary since operating 802.11 at higher rates results in drastically reduced efficiency and makes the measurements difficult to compare as the per-packet overhead dominates the overall cost. This is due

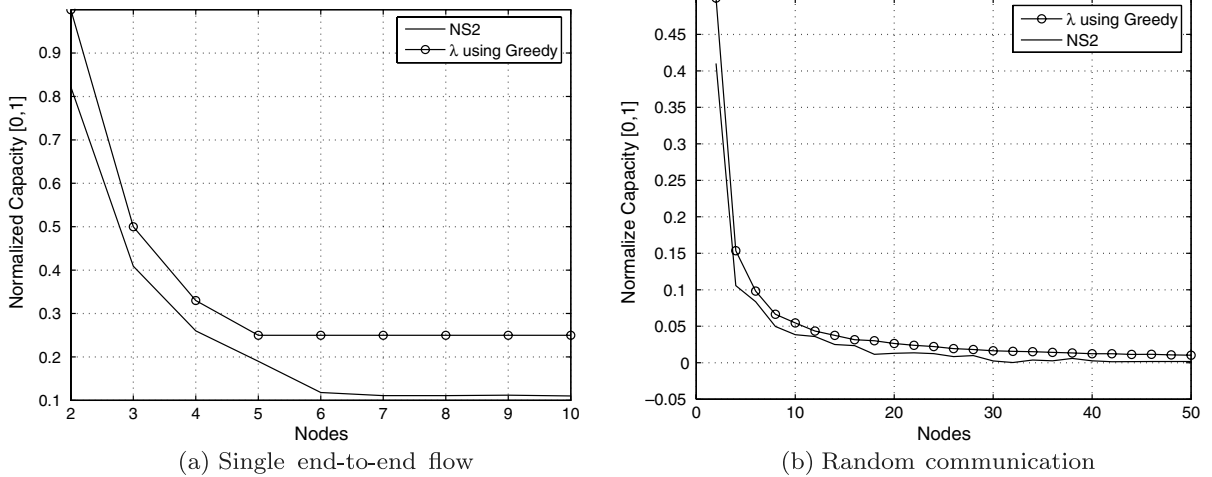


Fig. 3. Chain topology.

to the fixed length 802.11 preamble used by the hardware for bit synchronization.

7.1. Chain

In a first comparison we look at a configuration of a chain of n nodes. Each node is 200 m away from its neighbor. The first node acts as a source of data traffic, the last node is the traffic sink. Data is sent as fast as the MAC allows. We use *Greedy* as the channel assignment algorithm. Since there are no random components involved, λ is a direct function of the channels needed, and computes to $1/4$ as the chain grows. From Fig. 3a, we see that the value of λ lies above the throughput measured with ns-2, especially when the chain becomes large. This is due to the overhead of headers, RTS, CTS and ACK packets but also because in reality nodes fail to achieve an optimal schedule. The results obtained with our model match those presented in [13], where the authors discuss throughput capacity measurements taken from ns-2 simulations with respect to theoretical upper bounds.

As a more realistic scenario, we now investigate random communication patterns in chain topologies. For this purpose, we assign a random destination $d(n) \in \mathcal{N} \setminus \{n\}$ to every node $n \in \mathcal{N}$. Fig. 3b shows the effect of such a traffic pattern on throughput. The plot shows quite a close match between λ and the measurements obtained with ns-2. This is not too surprising since we know from Fig. 3a that the throughput of an 802.11 chain tallies with the theoretical limit if the chain length is short. Under a random communication pattern the average path

length in a chain is far below the maximum value of $n - 1$, for a chain of length n . Furthermore, overlapping communication paths reduce capacity ($B_{n,n'}$ in our model) due to the forwarding load inflicted upon the nodes, especially if the chain becomes long.

7.2. Grid

We look at grid topologies where each node is 200 m away from its closest neighbor and the nodes communicate using a random communication pattern. Fig. 4a shows the capacity in the grid topology for a cross communication pattern: source nodes in the first column have a destination assigned in the corresponding row in the last column, and source nodes in the first row have a destination assigned in the corresponding column in the last row. From Fig. 4a we see that the model based computation predicts a higher throughput capacity than the one measured with ns-2. This is because the cross communication pattern is actually composed of end-to-end chain communications exactly like the scenario used to compute Fig. 3a. We know that for large chain communications, 802.11 throughput capacity is far below the information-theoretic capacity,⁴ for reasons explained in Section 7.1. In the grid topology with cross communication this behavior is amplified. Fig. 4b shows the capacity in the grid for a random communication pattern

⁴ Information-theoretic capacity refers to the capacity that can be achieved with optimal routing and scheduling decisions, which possibly require global knowledge.

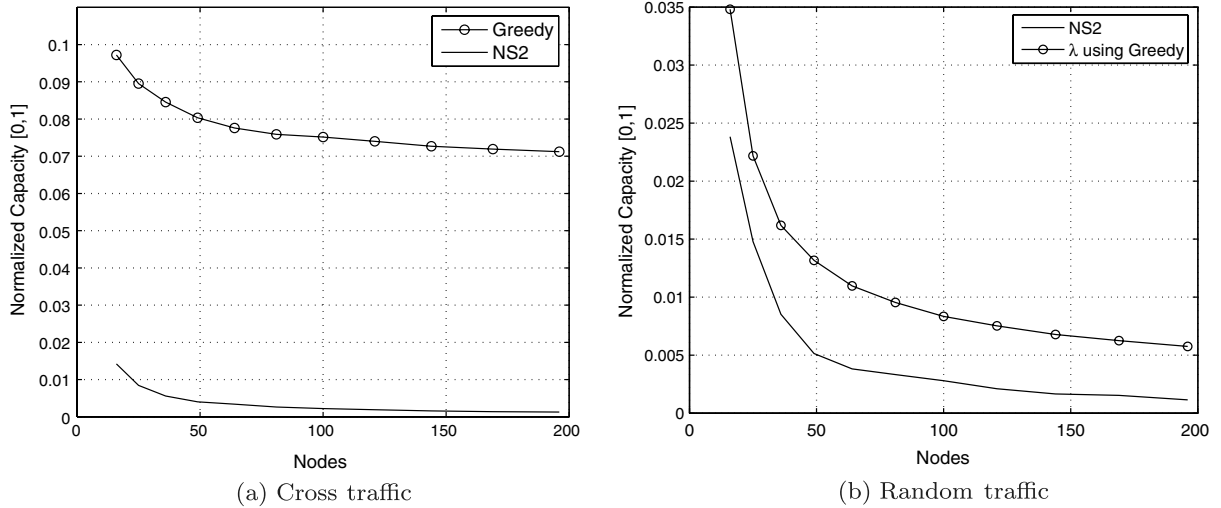


Fig. 4. Grid topology.

where each node gets assigned a random destination. Similarly to the chain example, the gap between ns-2 measurements and results obtained through our model disappears slightly when communication becomes random. Random communication reduces the average path length and therefore diminishes the impact of the suboptimal channel assignment and the header overhead inherent in 802.11.

7.3. Random topology

We consider random topologies of n nodes distributed uniformly within an area of $1000 \times$

1000 m^2 . Here, we have configured P_n^* such that the transmission range of the nodes equals 200 m. Each node n acts as a traffic generator and has a random destination assigned, chosen uniformly out of $\mathcal{N}\{n\}$. Fig. 5a shows the throughput capacity λ in contrast with ns-2 simulation measurements. The result supports the trend already observed in the previous configurations of the chain and the grid: randomness improves 802.11 throughput capacity with respect to λ . This might particularly be the case in dense networks where the demand for channels is high due to the high node degree, leaving less room for an optimal channel assignment.

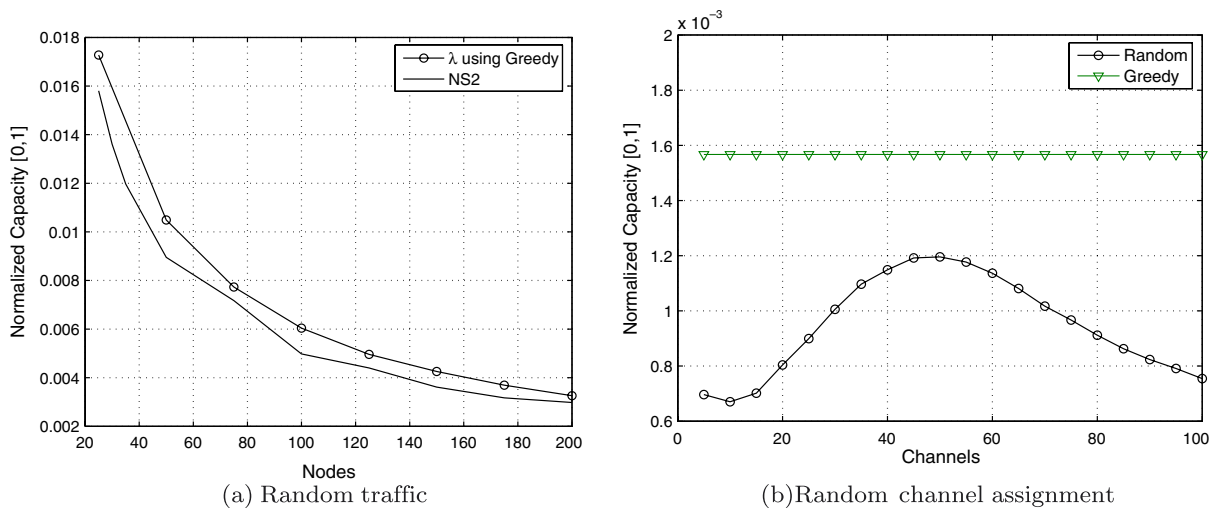


Fig. 5. Random topology.

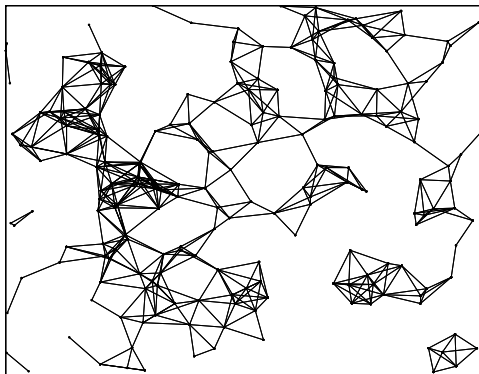
Algorithm 3. RandomEdge Channel AssignmentInput: The maximum number of channels T^* Output: Channel assignment ψ and number of used channels

```

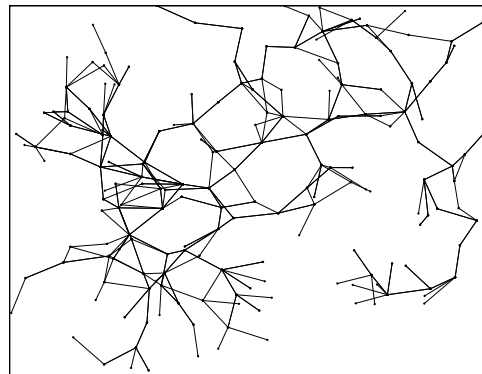
1:  $\mathcal{O} := \mathcal{E}$ ;
2:  $i := 0$ ;
3: while  $\mathcal{O} \neq \emptyset$  do
4:    $e := ANY\{e \in \mathcal{E}\}$ ;
5:    $\mathcal{O} := \mathcal{O} \setminus \{e\}$ ;
6:    $\psi(e) := i$ ;
7:    $i := (i + 1) \text{MOD } T^*$ ;
8: end while
9: if  $|\mathcal{N}| < T^*$  then
10:   return  $|\mathcal{N}|$ ;
11: else
12:   return  $T^*$ ;
13: end if

```

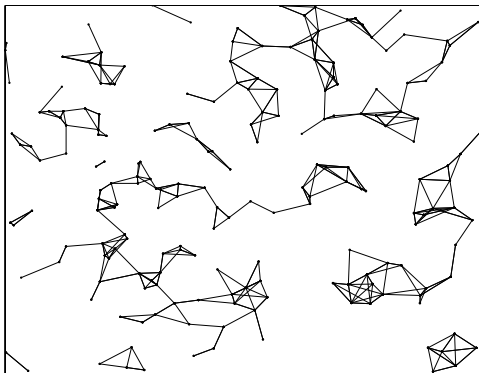
The model for throughput computation proposed in this work allows to easily exchange any of its components, such as, e.g., the scheduling algorithm or the radio propagation. In the following part, we will study the difference between a greedy channel assignment and a *random* channel assignment, with respect to throughput capacity. More particularly, we use the *RandomEdge* channel assignment (Algorithm 3), which assigns a set of maximum T channels in a round robin manner modulo T to all transmission pairs (n, n') with $n' \in \mathcal{D}_n$. At each round, one transmission pair is picked on a random basis. Fig. 5b shows the throughput capacity when using *RandomEdge* in a random topology of 200 nodes distributed within an area of $2000 \times 2000 \text{ m}^2$. We consider a random communication pattern. The result of Fig. 5b clearly shows that there is an optimum in terms of the



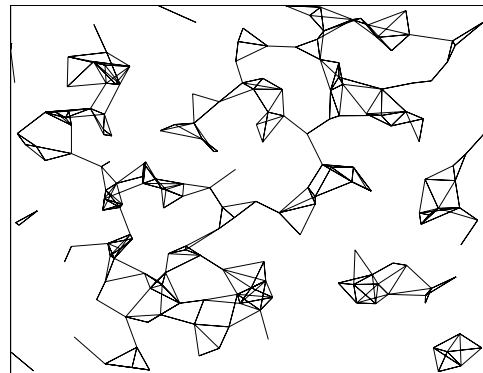
(a) Random network topology with 200 nodes



(b) Schedule graph under Greedy channel assignment



(c) Schedule graph under RandomEdge channel assignment with a maximum of 50 channels



(d) Schedule graph under RandomEdge channel assignment with a maximum of 80 channels

Fig. 6. Random networks and their schedule graphs under different channel assignment strategies.

number of channels T to be used when assigning them randomly to the transmissions. If only a few channels are used, all nodes transmit simultaneously and no transmission can be correctly decoded. If too many channels are used, most of the transmissions can actually be decoded, but since many transmissions are scheduled in separate channels, bandwidth is wasted. In fact, *RandomEdge* achieves a maximum throughput of about 0.0012 with an input set of around 50 channels, which is less than the throughput capacity of ≈ 0.0016 achieved by the *Greedy* channel assignment. Note that while *Greedy* assigns the channels in a conflict-free way, *RandomEdge* does not. This is also shown in Fig. 6 based on a snapshot of 200 nodes, distributed randomly within an area of $2000 \times 2000 \text{ m}^2$. Fig. 6a illustrates the random topology and Fig. 6b–d refers to the corresponding *schedule graphs* under the specific channel assignment algorithms. In the network graph, the dots represent the nodes and the edges represent the possible transmissions in the absence of interference (\mathcal{U}). The *schedule graph* in Fig. 6c is the result of a *RandomEdge* channel assignment using a fixed set of 50 channels (which in Fig. 5 was shown to be the optimum). As can be observed from Fig. 6b and c, *Greedy* (Algorithm 2) drops edges unused by the routing, but maintains full connectivity while *RandomEdge*, with 50 channels, produces a partially disconnected *schedule graph*. If we use more channels (Fig. 6d), the connectivity of the *schedule graph* improves, but more bandwidth is wasted due to the increase in the channels used.

7.4. Summary

Section 7 has shown that throughput capacity, computed based on the model proposed in this paper, can be used as a reasonable approximation for the potential throughput capacity of arbitrary network configurations. In general, the simulation results and the model based computations show a similar behavior. In most of the cases, the throughput capacity computed by the model is slightly higher than the one measured with ns-2. This, however, is natural since the ns-2 simulations are based on 802.11 which entails a suboptimal channel assignment and packet overhead. It is anyway important to note that the model should not be seen as a throughput capacity predictor for 802.11 based multihop wireless networks, but rather as an approximation of the potential throughput capacity of such a network in an information-theoretical sense.

8. Conclusions

In this work, we presented a model for studying throughput capacity of wireless multi-hop networks under realistic settings. Contrary to existing work, looking at capacity from an asymptotic perspective based on simplified network models (e.g., protocol interference, unidirectional links, perfect scheduling or straight line routing), our approach analyzes capacity for finite networks under more realistic network configurations. In our model, the effective throughput of a random network is considered as a random variable depending on the node distribution, the communication pattern, the radio propagation, channel assignment, etc. Expected values of that random variable are then computed using Monte-Carlo methods. The various components of the model can easily be exchanged to study any form of physical and logical interaction (e.g., shadow fading radio propagation, physical interference, random scheduling, etc.) with regard to throughput capacity. While the idea of treating throughput capacity as the expected value of a well modeled random variable serves as the basis for this work, the general concept can also be applied to other network properties. In that sense, the paper also suggests a new approach to ad hoc network analysis in cases where pure analytical approaches fall short and protocol specific network simulations are not generic enough. This is of particular importance considering the increasing computing power of today's hardware. For instance, although the computational costs of our model is $O(n^3)$, we were able to compute all the results within a few minutes using a cluster of 32 machines and JOpera [16] as a grid engine.

References

- [1] D. Aguayo, J. Bicket, S. Biswas, G. Judd, R. Morris, Link-level measurements from an 802.11b mesh network, SIGCOMM (2004).
- [2] P. Barbrand, D. Yuan, Maximal throughput of spatial tdma in ad hoc networks, in: 3rd Scandinavian Workshop on Wireless Ad-hoc Networks, 2003.
- [3] C. Bettstetter, C. Hartmann, Connectivity of wireless multihop networks in a shadow fading environment, in: MSWIM'03: Proceedings of the 6th ACM international workshop on Modeling analysis and simulation of wireless and mobile systems, ACM Press, New York, NY, USA, 2003, pp. 28–32.
- [4] P. Bjorklund, P. Varbrand, D. Yuan, Resource optimization of spatial tdma in ad hoc radio networks: a column generation approach, in: IEEE INFOCOM, March 2003.

- [5] G. Brar, D.M. Blough, P. Santi, Computationally efficient scheduling with the physical interference model for throughput improvement in wireless mesh networks, in: *MobiCom'06: Proceedings of the 12th Annual International Conference on Mobile Computing and Networking*, ACM Press, New York, NY, USA, 2006, pp. 2–13.
- [6] A. Brzezinski, G. Zussman, E. Modiano, Enabling distributed throughput maximization in wireless mesh networks: a partitioning approach, in: *MobiCom'06: Proceedings of the 12th Annual International Conference on Mobile Computing and Networking*, ACM Press, New York, NY, USA, 2006, pp. 26–37.
- [7] O. Dousse, P. Thiran, Connectivity vs capacity in dense ad hoc networks, in: *Proceedings of the of IEEE INFOCOM, Hong Kong, 2004*.
- [8] J. Gomez, A. Campbell, A case for variable-range transmission power control in wireless ad hoc networks, in: *IEEE INFOCOM, March 2004*.
- [9] P. Gupta, P. Kumar, Capacity of wireless networks, *Information Theory* 46 (2) (2000) 388–404.
- [10] A. Keshavarz-Haddad, V. Ribeiro, R. Riedi, Broadcast capacity in multihop wireless networks, in: *MobiCom'06: Proceedings of the 12th Annual International Conference on Mobile Computing and Networking*, ACM Press, New York, NY, USA, 2006, pp. 239–250.
- [11] S. Krumke, M. Marathe, Models and approximation algorithms for channel assignment in radio networks, *Wireless Networks* 7 (6) (2001) 575–584.
- [12] P. Kyasanur, N.H. Vaidya, Capacity of multi-channel wireless networks: impact of number of channels and interfaces, in: *MobiCom'05*, ACM Press, New York, NY, USA, 2005.
- [13] J. Li, C. Blake, D.S.D. Couto, H.I. Lee, R. Morris, Capacity of ad hoc wireless networks, in: *MobiCom'01*, ACM Press, New York, NY, USA, 2001.
- [14] H. Lim, C. Lim, J.C. Hou, A coordinate-based approach for exploiting temporal-spatial diversity in wireless mesh networks, in: *MobiCom'06: Proceedings of the 12th Annual International Conference on Mobile Computing and Networking*, ACM Press, New York, NY, USA, 2006, pp. 14–25.
- [15] T. Moscibroda, R. Wattenhofer, A. Zollinger, Topology control meets sinr: the scheduling complexity of arbitrary topologies, in: *MobiHoc'06: Proceedings of the Seventh ACM International Symposium on Mobile Ad hoc Networking and Computing*, ACM Press, New York, NY, USA, 2006, pp. 310–321.
- [16] Pautasso C. Pautasso, JOpera: an agile environment for web service composition with visual unit testing and refactoring, in: *VL/HCC*, IEEE Computer Society, 2005, pp. 311–313. www.jopera.ethz.ch.
- [17] S. Ramanathan, E.L. Lloyd, Scheduling algorithms for multihop radio networks, *IEEE/ACM Transactions on Networks* 1 (2) (1993) 166–177.
- [18] T.S. Rappaport, *Wireless Communications: Principles & Practice*, Prentice-Hall, Englewood Cliffs, New Jersey, 2002.
- [19] G. Sharma, R.R. Mazumdar, N.B. Shroff, On the complexity of scheduling in wireless networks, in: *MobiCom'06: Proceedings of the 12th Annual International Conference on Mobile Computing and Networking*, ACM Press, New York, NY, USA, 2006, pp. 227–238.
- [20] P. Soldati, B. Johansson, M. Johansson, Proportionally fair allocation of end-to-end bandwidth in stma wireless networks, in: *MobiHoc'06: Proceedings of the Seventh ACM International Symposium on Mobile Ad hoc Networking and Computing*, ACM Press, New York, NY, USA, 2006, pp. 286–297.
- [21] M. Takai, J. Martin, R. Bagrodia, Effects of wireless physical layer modeling in mobile ad hoc networks, in: *MobiHoc'01: Proceedings of the 2nd ACM International Symposium on Mobile Ad hoc Networking & Computing*, ACM Press, New York, NY, USA, 2001, pp. 87–94.
- [22] The VINT Project. The NS network simulator, <http://www.isi.edu/nsnam/ns>, 2002.
- [23] S. Toumpis, A. Goldsmith, Capacity regions for wireless adhoc networks (2001).
- [24] W. Wang, X.-Y. Li, O. Frieder, Y. Wang, W.-Z. Song, Efficient interference-aware tdma link scheduling for static wireless networks, in: *MobiCom'06: Proceedings of the 12th Annual International Conference on Mobile Computing and Networking*, ACM Press, New York, NY, USA, 2006, pp. 262–273.
- [25] G. Zhou, T. He, S. Krishnamurthy, J.A. Stankovic, Impact of radio irregularity on wireless sensor networks, in: *MobiSys'04: Proceedings of the 2nd International Conference on Mobile Systems, Applications, and Services*, ACM Press, New York, NY, USA, 2004, pp. 125–138.
- [26] M. Zorzi, S. Pupolin, Optimum transmission ranges in multihop packet radio networks in the presence of fading, *IEEE Transactions on Communication* 43 (7) (1995).



Patrick Stuedi received a Diploma in Computer Science from the Swiss Federal Institute of Technology (ETH), Zurich in 2003. He is currently a Ph.D. student at the Institute of Pervasive Computing at ETH. His research interests are in fundamental properties of ad hoc networks, VoIP and QoS.



Gustavo Alonso is a Professor in the Department of Computer Science of ETH Zurich where is the Head of the Institute for Pervasive Computing and leads the Information and Communications Research Group. His research interest include distributed systems, adaptive software, web services and service oriented architecture, wireless sensor networks, and software systems in general. For more information on his research and his group, check: www.iks.inf.ethz.ch.